Post-Disaster Dispatch of Transportable Wind Turbines for Enhancing Resilience of Power Distribution Systems

Jinshun Su* and Payman Dehghanian†
Department of Electrical and Computer Engineering
The George Washington University
Washington, DC 20052, USA.
{*jsu66, †payman}@gwu.edu

2024 IEEE Texas Power and Energy Conference (TPEC) | 979-8-3503-3120-2/24/$31.00 ©2024 IEEE | DOI: 10.1109/TPEC60005.2024.10472177

***Abstract*—In the face of heightened societal interest in decarbonization, wind energy is emerging more and more as a viable, low-emission source of clean power. Unlike stationary wind turbines, mobile wind turbines (MWTs) possess the ability to be transported by truck, supplying electricity to power distribution systems (DSs). This spatiotemporal flexibility offers notable advantages, especially in enhancing system resilience following extreme natural disasters. However, the full potential of these resources remains untapped, underscoring the need for enhanced utilization strategies. In this paper, we develop an optimal scheme for strategically dispatching MWTs to enhance the resilience of the DS accounting for the uncertain predictions of wind energy. A joint chance-constrained programming (JCCP) model formulated as a mixed-integer nonlinear programming (MINLP) problem is introduced to capture the uncertainty in wind energy forecasts. We develop a linearization method that are computationally feasible, allowing us to transform the MINLP model into an equivalent mixed-integer linear programming (MILP) formulation. Case studies conducted on the IEEE 123-node test system illustrate the efficiency of the suggested service restoration strategy in enhancing the resilience of the DS during extreme events.**

***Index Terms*—Mobile wind turbine (MWT); joint chance-constrained programming (JCCP); wind energy forecasts; service restoration.**

NOMENCLATURE

A. Sets

$\mathbf{T}$	Time periods.
$\mathbf{I}$	Nodes in the distribution system (DS).
$\mathbf{L}$	Lines in the DS.
$\mathbf{S}$	Segments in the DS.
$\mathbf{I}^c \subset \mathbf{I}$	Candidate nodes in the DS.
$\mathbf{I}^s \subset \mathbf{I}$	Substation nodes in the DS.
$\mathbf{M}$	Mobile wind turbines (MWTs).
$\mathbf{H}$	Hydrogen storage units (HSUs).

B. Parameters

α_i	Value of lost load at node i.
β_t	Cost of energy not provided by the electric utility at time t.
C_i	Capacity of candidate node i for hosting MWTs.
D^a_{it}, D^r_{it}	Amount of active/reactive power demand at node i at time t.
T^m_{ij}	Travel time from node i to j with MWT m.
δ_{is}	Indicator denoting whether candidate node i belongs to segment s.
W_m	Wind power capacity of MWT m.
λ_{lt}	Indicator denoting whether power line l is energized at time t.
F^a_l, F^r_l	Active/Reactive power limit of line l.
R_l, X_l	Resistance/Reactance of line l.
U	Big M number.
$\underline{V}_i, \overline{V}_i$	Minimum/Maximum squared voltage magnitude at node i.
G^a, G^r	Active/Reactive power capacity of substation.
$\hat{\delta}_{ih}$	Indicator denoting whether HSU h is installed at node i.
$\underline{\theta}_i, \overline{\theta}_i$	Lower/Upper bound of power factor angle at node i.
$\underline{E}_h, \overline{E}_h$	Lower/Upper bound of hydrogen storage level (HEL) of HSU h.
$\eta_h, \tilde{\eta}_h$	Hydrogen-to-power (H2P)/Power-to-Hydrogen (P2H) efficiency of HSU h.
$Z_h, \tilde{Z}_h$	Limit of consumed/generated power of HSU h in H2P/P2H mode.

C. Decision and Random Variables

x_{mit}	Binary variable equal to 1 if MWT m is connected to candidate node i at time t.
y^a_{it}, y^r_{it}	Fraction of active/reactive power outage at node i at time t.
w_{imt}	Power supplied by each MWT m to node i at time t.
f^a_{lt}, f^r_{lt}	Active/Reactive power flow in line l at time t.
ϕ^a_{it}, ϕ^r_{it}	Total active/reactive power delivery to node i at time t.
v_{it}	Squared voltage magnitude at node i at time t.
$z_{ht}, \tilde{z}_{ht}$	Generated/Consumed power of HSU h in H2P/P2H mode at time t.
E_{ht}	HEL of HSU h at time t.
$\mu_{ht}, \tilde{\mu}_{ht}$	Binary variable equal to 1 if HSU h is in H2P/P2H mode at time t.
ξ_{st}	Random variable of predicted wind energy in segment s at time t.

979-8-3503-3120-2/24/$31.00©2024 IEEE

I. Introduction

In recent years, the rise in extreme natural disasters like wildfires, hurricanes, and floods has led to significant equipment damage, extended power outages, considerable economic losses, and widespread disruption to contemporary society [1]. For example, the United States witnessed more than 200,000 wildfire incidents between 2017 and 2020, which ravaged over 25 million acres of land [2]. In addition, the 2017 Hurricane Harvey caused significant power outages (10,000 MW) and left more than 291,000 people without electricity [3]. The rising frequency of these extreme natural disasters can be attributed to climate change, underscoring the importance of establishing sustainable energy systems as a crucial measure to alleviate the effects of climate change-induced extreme natural disasters.

Taking into account environmental factors, there has been extensive adoption and integration of renewable and eco-friendly energy sources in current power systems [4]–[6]. The swift integration of renewable energy resources substantially achieves decarbonization and enhances the power grid resilience against extreme natural disasters [7]. For example, [8] presents an adaptive robust optimization approach that aims to expedite and ensure a self-healing process by synchronizing the operations of wind farms and pumped-storage hydro units. Reference [9] proposes a security-constrained economic dispatch model for seaport energy management via integrating hydrogen resources.

Relative to statically-positioned renewable energy resources such as wind turbines [10], photovoltaics [11], and hydrogen storage units (HSUs) [12], [13], the application of mobile power sources (MPSs) presents a notable opportunity to facilitate spatiotemporal flexibility exchange within the distribution system (DS). This potential enhancement can contribute to bolstering system resilience and optimizing overall efficiency. For example, the research detailed in [14] suggests a two-stage approach for restoring DSs, which fully utilizes the dispatch of MPSs in combination with dynamic distribution network reconfiguration across various seismic force scenarios. A novel DS restoration mechanism for the use of MPSs jointly operated with stochastic solar and wind energy sources, that captures the corresponding uncertainties with joint probabilistic constraints is developed in [15]. The study in [16] takes into account the endogenous uncertainty related to the presence of MPSs, to provide a more realistic assessment of how MPSs contribute to enhancing the resilience of the DS. Reference [17] develops a risk management model for the strategic placement of MPSs and public safety power-shutoff actions, focusing on equilibrating risks of wildfire and power-shutoff-induced power interruption in the DS.

However, the investigation of MPSs in the literature [14]–[17] reveals their reliance on traditional energy sources for power supply, resulting in elevated operational expenses and environmentally detrimental emissions. Mobile wind turbines (MWTs), known for their compactness and portability, are small-scale wind energy devices designed for easy transportation, commonly used for power generation in areas not connected to the grid or in isolated locations. Reference [18] integrates the combined use of MWTs and electric thermal storage into the energy portfolio, enabling load profile modification and avoiding costs linked to peak demand. With their capacity for spatiotemporal adaptability, MWTs emerge as a compelling option for delivering emergency energy to DSs in the face of severe weather conditions. For example, the study [19] develops a two-stage stochastic model to enhance system resilience via pre-positioning of MWTs.

Fig. 1. A state-of-the-art mobile wind turbine setup [20].

As far as we are aware, analytical models are absent in existing literature for the dispatch of MWTs for service restoration. To bridge this gap, we introduce a new restoration approach that encompasses the coordination of MWTs' routing and scheduling, along with the management of HSUs. A nonlinear joint chance-constrained programming (JCCP) model is formulated to solve the proposed service restoration scheme under uncertainty in predicted wind energy. The model performance is tested and numerically verified on the IEEE 123-node test system.

The remainder of the paper is structured in the following way: Section II introduces the proposed service restoration model with JCCP formulation. Section III describes the method to reformulate the proposed nonlinear formulation to an equivalent linear model. Section IV presents the numerical results, while Section V provides a conclusion of the research findings.

II. Proposed Methodology

We here present a post-disaster service restoration model (**SRM**), which accounts for the deployment of MWTs under the uncertainty of wind energy and the operation of HSUs. The introduced scheme is formulated as a stochastic mixed-integer nonlinear programming (MINLP) problem with the following objective function:

$$\min \sum_{i\in\mathbf{I}} \sum_{t\in\mathbf{T}} (\alpha_i + \beta_t) D^a_{it} y^a_{it} \tag{1}$$

The goal of the objective function (1) is to reduce the overall costs associated with power interruptions, encompassing both the costs of disrupted energy for each node and energy not sold by the electric utility at each time. The proposed optimization model features a mixed-integer nonlinear framework, delineated by the constraints outlined in subsequent subsections II-A - II-D.

A. MWTs Allocation and Operation Constraints

Constraint (2a) imposes a limitation on how many MWTs can be assigned at each candidate node. Each MWT is allowed to reside at only 1 node at any given period (see constraint (2b)). Constraint (2c) denotes the deployment of MWTs. Constraint (2d) implies the joint chance constraints in which the probability that the available wind energy could be used by MWTs in each DS segment satisfies a predefined reliability level ϵ. Constraint (2e) stipulates that the power supplied by MWT m in a candidate node does not surpass its designated capacity when it is connected. There is no power output from MWTs in non-candidate nodes (see constraint (2f)).

$$\sum_{m\in\mathbf{M}} x_{mit} \le C_i, \qquad i\in\mathbf{I}^c, t\in\mathbf{T} \quad (2a)$$

$$\sum_{i\in\mathbf{I}^c} x_{mit} \le 1, \qquad m\in\mathbf{M}, t\in\mathbf{T} \quad (2b)$$

$$x_{mi(t+\tau)} \le 1 - x_{mjt}, \qquad m\in\mathbf{M}, i,j\in\mathbf{I}^c, \tau\le T^m_{ij}, t\le|\mathbf{T}|-\tau \quad (2c)$$

$$\mathbb{P}\Big(\sum_{m\in\mathbf{M}} w_{mit}\delta_{is} \le \xi_{st}, s\in\mathbf{S}\Big) \ge \epsilon, \qquad i\in\mathbf{I}^c, t\in\mathbf{T} \quad (2d)$$

$$0 \le w_{mit} \le W_m x_{mit}, \qquad m\in\mathbf{M}, i\in\mathbf{I}^c, t\in\mathbf{T} \quad (2e)$$

$$w_{mit} = 0, \qquad m\in\mathbf{M}, i\in\mathbf{I}\setminus\mathbf{I}^c, t\in\mathbf{T} \quad (2f)$$

B. Power Balance Constraints

Constraints (3a) and (3b) describe the active and reactive power balance conditions at each DS node. Notations $\Theta(l)$ and $\Gamma(l)$ represent the parent and child nodes belonging to each power line in the DS. Constraints (3c) and (3d) establish the limits for active and reactive power injection at the substation node of the DS. The setting of active and reactive power delivery to nodes other than the substation is determined by constraints (3e) and (3f).

$$\sum_{l\in\mathbf{L}_\phi;\Theta(l)=i} f^a_{lt} + D^a_{it}(1-y^a_{it}) = \sum_{l\in\mathbf{L}_\phi;\Gamma(l)=i} f^a_{lt} + \phi^a_{it}, \qquad i\in\mathbf{I}, t\in\mathbf{T} \quad (3a)$$

$$\sum_{l\in\mathbf{L}_\phi;\Theta(l)=i} f^r_{lt} + D^r_{it}(1-y^r_{it}) = \sum_{l\in\mathbf{L}_\phi;\Gamma(l)=i} f^r_{lt} + \phi^r_{it}, \qquad i\in\mathbf{I}, t\in\mathbf{T} \quad (3b)$$

$$0 \le \phi^a_{1t} \le G^a, \qquad t\in\mathbf{T} \quad (3c)$$

$$0 \le \phi^r_{1t} \le G^r, \qquad t\in\mathbf{T} \quad (3d)$$

$$\phi^a_{it} = \sum_{h\in\mathbf{H}} (z_{ht} - \tilde{z}_{ht})\hat{\delta}_{ih} + \sum_{m\in\mathbf{M}} w_{mit}, \qquad i\in\mathbf{I}\setminus\{1\}, t\in\mathbf{T} \quad (3e)$$

$$\phi^a_{it}\tan\underline{\theta}_i \le \phi^r_{it} \le \phi^a_{it}\tan\overline{\theta}_i, \qquad i\in\mathbf{I}\setminus\{1\}, t\in\mathbf{T} \quad (3f)$$

C. Power Flow Constraints

Constraints (4a) and (4b) stipulate the active and reactive power flows in the connected power lines, and force the value of power flows to be 0 in disconnected power lines. Constraints (4c) and (4d) denote the power flow equations where the term $U(\lambda_{lt}-1)$ or $U(1-\lambda_{lt})$ guarantees the satisfaction of the power flow condition across functional lines based on the DistFlow model [15]. Constraint (4e) represents the limits on the squared voltage magnitude of each node at any given period.

$$-\lambda_{lt}F^a_l \le f^a_{lt} \le \lambda_{lt}F^a_l, \qquad l\in\mathbf{L}, t\in\mathbf{T} \quad (4a)$$

$$-\lambda_{lt}F^r_l \le f^r_{lt} \le \lambda_{lt}F^r_l, \qquad l\in\mathbf{L}, t\in\mathbf{T} \quad (4b)$$

$$v_{it} - v_{jt} \le 2(R_l f^a_{lt} + X_l f^r_{lt}) + U(1-\lambda_{lt}), \qquad i,j\in\mathbf{I}, l\in\mathbf{L}, t\in\mathbf{T} \quad (4c)$$

$$v_{it} - v_{jt} \ge 2(R_l f^a_{lt} + X_l f^r_{lt}) + U(\lambda_{lt}-1), \qquad i,j\in\mathbf{I}, l\in\mathbf{L}, t\in\mathbf{T} \quad (4d)$$

$$\underline{V}_i \le v_{it} \le \overline{V}_i, \qquad i\in\mathbf{I}, t\in\mathbf{T} \quad (4e)$$

D. HSSs Operation Constraints

To enable efficient storage and use of renewable energy resources, hydrogen storage units are considered in the restoration process. The change in HELs of HSU h over time is governed by their hydrogen-to-power (H2P) and power-to-hydrogen (P2H) activities, as specified in constraint (5a). Constraint (5b) sets the limits for the HEL in HSU h. The output limits of HSUs in H2P and P2H modes are detailed in constraints (5c) and (5d), respectively. Constraint (5e) mandates that the H2P and P2H modes of HSU h cannot operate simultaneously.

$$E_{h(t+1)} = E_{ht} + (\tilde{z}_{ht}\tilde{\eta}_h - z_{ht}/\eta_h), \qquad h\in\mathbf{H}, t\in\mathbf{T}\setminus\{|\mathbf{T}|\} \quad (5a)$$

$$\underline{E}_h \le E_{ht} \le \overline{E}_h, \qquad h\in\mathbf{H}, t\in\mathbf{T} \quad (5b)$$

$$0 \le z_{ht} \le Z_h\mu_{ht}, \qquad h\in\mathbf{H}, t\in\mathbf{T} \quad (5c)$$

$$0 \le \tilde{z}_{ht} \le \tilde{Z}_h\tilde{\mu}_{ht}, \qquad h\in\mathbf{H}, t\in\mathbf{T} \quad (5d)$$

$$\mu_{ht} + \tilde{\mu}_{ht} \le 1, \qquad h\in\mathbf{H}, t\in\mathbf{T} \quad (5e)$$

III. Solution Method

The joint chance constraint introduced in equation (2d) delineates a feasible region characterized by nonlinearity, which implies that model **SRM** is not convex regardless of the integrality restrictions on Several decision variables. We now drive mixed-integer linear programming (MILP) reformulation equivalent to model (5). Proposition 1 shows the process of linearizing the nonlinear terms in the MINLP model when a scenario-based reformulation is applied.

Proposition 1: Let $\gamma^k \in \{0,1\}^k$ be the auxiliary decision variables. The MILP reformulation problem **R-SRM**

$$\min \sum_{i\in\mathbf{I}}\sum_{t\in\mathbf{T}} (\alpha_i + \beta_t) D^a_{it} y^a_{it} \quad (6a)$$

$$\text{s.to. (2a)} - \text{(2c)},\ \text{(2e)} - \text{(5e)} \quad (6b)$$

$$-\sum_{m\in\mathbf{M}} w_{mit}\delta_{is} \ge \omega^k_{st}(1-\gamma^k), \qquad k\in\mathbf{\Omega}, i\in\mathbf{I}^c, s\in\mathbf{S}, t\in\mathbf{T} \quad (6c)$$

$$\sum_{k\in\Omega} p^k\gamma^k \le 1-\epsilon \qquad i\in\mathbf{I}^c, t\in\mathbf{T} \quad (6d)$$

is equivalent to model **SRM**.

Proof. Consider a general JCCP model with a linear objective function as follows:

$$\min\ q^T X \tag{7a}$$
$$\text{s.to. } AX \geq b \tag{7b}$$
$$\mathbb{P}(h_j X \geq \xi_j, \quad j \in \mathbf{J}) \geq \epsilon \tag{7c}$$
$$X \geq 0 \tag{7d}$$

where ξ_j defines a vector of random variables following an $|\mathcal{J}|$-dimensional distribution with finite support and ϵ defines a global reliability level for constraint (7c). Constraint (7b) indicates the linear feasible region of the model (7). Based on the scenario-based formulation presented in [21], the joint chance constraint (7c) satisfies the constraints defined over set $\mathbf{J}$ holistically with global reliability level p. Let notation Ω be the set of scenarios, and ω_j^k denote the realization of random variable ξ_j in scenario k. The probability of each scenario is denoted by p^k. By defining a binary variable γ^k for each ω_j^k, the reformulation model is described below:

$$\min\ q^T X \tag{8a}$$
$$\text{s.to. } AX \geq b \tag{8b}$$
$$h_j X \geq \omega_j^k (1-\gamma^k), \qquad j \in J, k \in \Omega \tag{8c}$$
$$\sum_{k\in\Omega} p^k \gamma^k \leq 1-\epsilon \tag{8d}$$
$$X \geq 0. \tag{8e}$$

Now, we introduce ω_{st}^k to represent the realization of the forecasted wind energy in DS segment s at time t in scenario k. Derived by constraints (8c) and (8d), the nonlinear chance constraint (2d) can be reformulated by constraints (6c) and (6d).

The problem (objective function and all constraints) is then linear, which provides the result we set out to prove. □

IV. Numerical Analyses

A. System Description

The application of the introduced model and solution technique to the IEEE 123-node test system is presented in this Section. The IEEE 123-node test system owns 1 substation, 123 nodes, and 122 lines (See Fig. 2), further information on which is available in [22]. In this study, the IEEE 123-node test system is assumed to host 15 candidate nodes and 6 HSUs. Six MWTs of 300 kW capacity are planned to be used in the system restoration which is considered, in all tests, to last for 12 hours in 48 periods of 15-minute duration. As a medium-size DS [23], we partition the IEEE 123-node test system into three segments, each featuring distinct realizations of wind energy for the same period. Monte Carlo simulation is utilized to generate 100 scenarios that capture the realizations of wind energy in different segments of the DS following the Weibull distribution [24].

The role of joint utilization of MWTs and HSUs on the DS performance resilience is investigated through three different cases described as follows:

- **Case I**: five lines are damaged by an incident;
- **Case II**: eight lines are damaged by an incident;
- **Case III**: twelve lines are damaged by an incident.

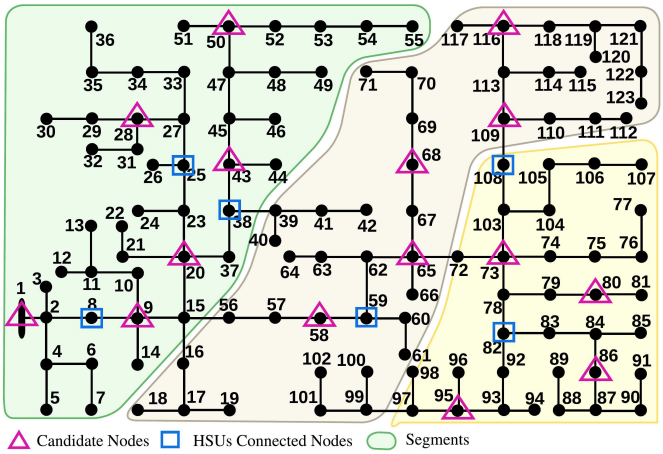

Fig. 2. The studied IEEE 123-node test system.

Numerical experiments were conducted on a PC with an Intel i7-8700 processor and 32 GB of RAM. We used AMPL to formulate the optimization problem, which was then solved using the Gurobi 10.0.0 optimization solver.

B. Analysis and Discussions

In all cases, the damaged power lines are assumed to be repaired within 12 hours, which is indicated by λ_{lt}. Figure 3 illustrates a comparative analysis of the percentage of restored demand over 12 hours for three different cases, both with and without the use of MWTs. In each case, the inclusion of MWTs leads to a more rapid and higher portion of demand restoration. For instance, **Case I** illustrates that without MWTs, demand restoration remains at 5% throughout the period, whereas with MWTs, it progressively increases from 40% in the first hour to complete restoration by the 9th hour. In **Case II**, there's a consistent rise in DS restoration, achieving full demand recovery by the 11th hour with MWTs. **Case III**'s restoration trajectory is similar to **Case I** and **Case II** with MWTs. Overall, each case achieves or approaches full DS restoration with MWTs, contrasting sharply with the scenarios without MWTs, where DS restoration is markedly less efficient. This emphasizes the effectiveness of MWTs in enhancing the DS restoration capacity over time, particularly in scenarios that might represent different levels of initial damage, available resources, or other varying conditions that could affect restoration efforts.

Subsequently, we turn our attention to evaluating the impact of MWTs on decarbonization efforts by contrasting their performance with that of conventional transportable emergency generators (TEGs). In particular, we scrutinize the efficacy of six TEGs, each rated at 300 kW, in both restoring service and facilitating decarbonization, while ensuring the conditions remain constant across all the cases studied. Furthermore, we explore a hybrid approach that leverages the combined advantages of both MWTs and TEGs. In this scenario, we integrate three MWTs with an equivalent number of TEGs, adhering to the uniform settings applied in the previously studied cases. This examination aims to discern the potential synergies that may arise from the concurrent use of MWTs

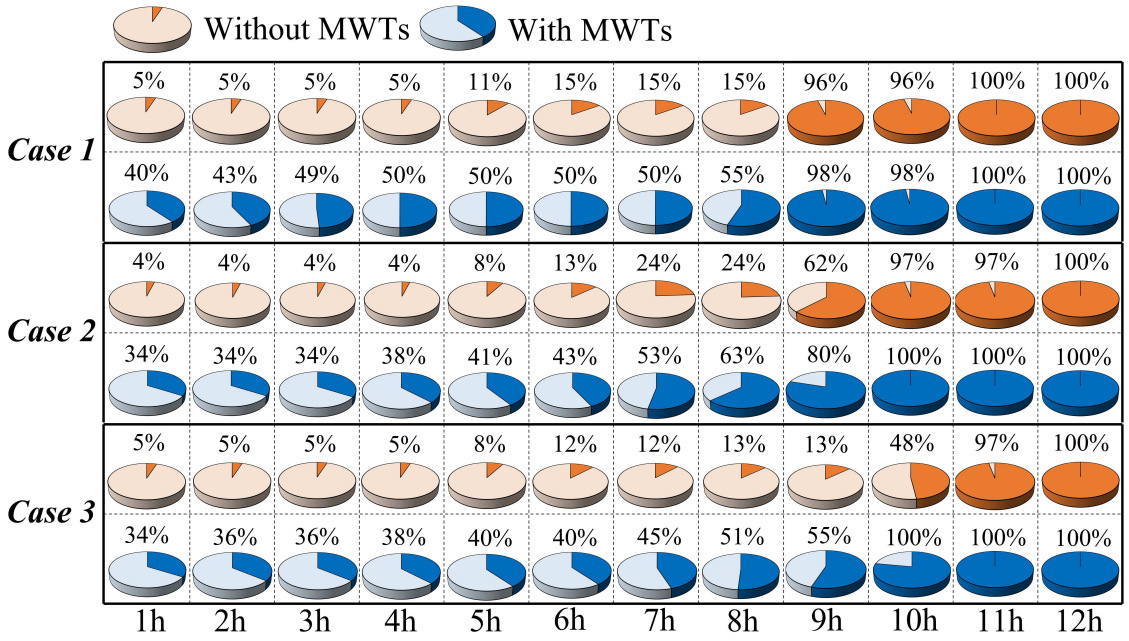

Fig. 3. The total restored load by the restoration horizon in different cases with and without MWTs.

and TEGs in enhancing DS service restoration while also advancing decarbonization objectives. We calculate the carbon dioxide (CO_2) emissions produced by the operation of TEGs during the restoration process, using data from the U.S. Environmental Protection Agency report [25].

Table I illustrates the CO_2 emissions and costs associated with power outages when MWTs and TEGs are utilized. The term "No MPSs" in the table refers to the scenario without considering any MPSs (i.e., MWTs and TEGs) for DS service restoration in all studied cases. According to Table I, several observations can be made:

- In all three cases, the utilization of different types of MPS technologies leads to a significant reduction in total outage costs when compared to scenarios without using MPSs, with savings ranging from approximately 51% to 86%;
- CO_2 emissions are eliminated when MWTs are used alone, highlighting their environmental advantage, although this approach, while reducing outage costs compared to no MPSs scenario, is the less cost-effective option among the strategies considered, with the smallest reduction in outage costs.
- TEGs alone provide the most significant reduction in outage costs across all cases but lead to the highest CO_2 emissions.
- The hybrid approach ("Mix") of combining MWTs and TEGs yields a significant reduction in CO_2 emissions compared to using TEGs alone, cutting emissions by roughly 54% to 57% across the studied cases. Although it still results in CO_2 emissions, it is more cost-effective in service restoration than using MWTs alone.

Utilizing MWTs alone provides a desirable decarbonization practice but is less cost-effective while using TEGs alone offers the greatest cost savings but also the highest CO_2 emissions. The hybrid approach balances both, cutting emissions substantially while offering greater cost efficiency than MWTs alone. Operators should weigh these considerations against their specific priorities, whether they be financial, environmental, or a balance of both, to make an informed decision on the deployment of MPSs in disaster-struck areas.

TABLE I
PERFORMANCE OF MWTS, TYPICAL TEGS, AND THE HYBRID APPROACH

		Case I	Case II	Case III
Total Outage Costs ($)	**No MPSs**	17,629k	17,996k	21,439k
	MWTs	8,443k	9,790k	11,610k
	TEGs	2,485k	6,710k	7,791k
	Mix	5,207k	7,521k	8,053k
CO_2 **Emission** (*ton*)	**MWTs**	0	0	0
	TEGs	19.08	21.13	23.49
	Mix	8.87	10.02	11.37

Next, we evaluate the impact of HSUs on DS service restoration. Table II offers a summary of the results for all investigated cases with and without consideration of using HSUs. In the table, "Non-Use" refers to scenarios where neither MWTs nor HSUs are employed, while "Both" denotes scenarios where a combination of MWTs and HSUs is implemented. Table II showcases the benefits of integrating MWTs with HSUs in reducing unserved energy and wind curtailment across three studied cases. The combined use of MWTs and HSUs consistently results in the least energy not served, indicating the hybrid strategy's effectiveness in enhancing power delivery. Moreover, the expected wind curtailment percentage is dramatically higher when neither technology is utilized. The integration of MWTs alone mitigates wind curtailment substantially, but the most significant reduction is achieved when MWTs and HSUs are used jointly. The results suggest that the combination of MWTs and HSUs could provide a

more resilient and efficient solution to energy challenges in the DS particularly when facing extreme events.

TABLE II
SUMMARY OF THE IMPACT OF HSUS ON DS RESTORATION

		Case I	Case II	Case III
Energy Not Served (*kWh*)	**Non-Use**	17,428	18,066	21,047
	MWTs Only	12,756	13,778	16,721
	Both	9,925	11,209	13,102
Expected Wind Curtailment Percentage (%)	**Non-Use**	100	100	100
	MWTs Only	56.52	55.31	54.87
	Both	32.18	30.77	29.12

V. CONCLUSION

We proposed a new service restoration mechanism that helps improve the resilience of the DS by making informed decisions on the dispatch of MWTs, jointly operating with HSUs. In order to capture the uncertainty in wind energy prediction, the introduced problem is formulated as a JCCP model and takes the form of a stochastic MINLP optimization problem. An efficient linearization method is designed to reformulate it as an equivalent MILP formulation. Numerical results on the IEEE 123-node test system emphasized the benefit and efficacy of the proposed approach for the DS resilience improvement against extreme natural disasters while reducing carbon emissions. The analyses of the results provide insights into how more informed decisions could be made on the joint utilization of MWTs and TEGs based on considerations against specific priorities, such as cost-effectiveness, environmental impact, and a balance of both. Future research could enhance the decision-making process by incorporating an assessment of the transportation network's condition and availability in the aftermath of an extreme disaster.

VI. ACKNOWLEDGMENT

This work was supported in part by the U.S. National Science Foundation (NSF) under Grants RISE-2220626 and ECCS-2114100.

REFERENCES

[1] J. Su, P. Dehghanian, M. Nazemi, and B. Wang, "Distributed wind power resources for enhanced power grid resilience," in *2019 North American Power Symposium (NAPS)*, pp. 1–6, 2019.

[2] M. Nazemi, P. Dehghanian, Y. Darestani, and J. Su, "Parameterized wildfire fragility functions for overhead power line conductors," *IEEE Transactions on Power Systems*, 2023.

[3] D. Anokhin, P. Dehghanian, M. A. Lejeune, and J. Su, "Mobility-as-a-service for resilience delivery in power distribution systems," *Production and Operations Management*, vol. 30, no. 8, pp. 2492–2521, 2021.

[4] S. Wang, P. Dehghanian, M. Alhazmi, J. Su, and B. Shinde, "Resilience-assured protective control of DC/AC inverters under unbalanced and fault scenarios," in *2019 IEEE Power & Energy Society Innovative Smart Grid Technologies Conference (ISGT)*, pp. 1–5, 2019.

[5] N. Shi, R. Cheng, L. Liu, Z. Wang, Q. Zhang, and M. J. Reno, "Data-driven affinely adjustable robust Volt/VAr control," *IEEE Transactions on Smart Grid*, pp. 1–1, 2023.

[6] J. Chen, W. Wu, and L. A. Roald, "Data-driven piecewise linearization for distribution three-phase stochastic power flow," *IEEE Transactions on Smart Grid*, vol. 13, no. 2, pp. 1035–1048, 2021.

[7] X. Huo, J. Dong, B. Cui, B. Liu, J. Lian, and M. Liu, "Two-level decentralized-centralized control of distributed energy resources in grid-interactive efficient buildings," *IEEE Control Systems Letters*, vol. 7, pp. 997–1002, 2023.

[8] A. Golshani, W. Sun, Q. Zhou, Q. P. Zheng, J. Wang, and F. Qiu, "Coordination of wind farm and pumped-storage hydro for a self-healing power grid," *IEEE Transactions on Sustainable Energy*, vol. 9, no. 4, pp. 1910–1920, 2018.

[9] C. Xie, J. Su, and P. Dehghanian, "Optimal energy scheduling in seaport integrated energy systems," in *2023 IEEE PES GTD International Conference and Exposition (GTD)*, pp. 376–380, 2023.

[10] P. Huang and L. Vanfretti, "Multi-tuned narrowband damping for suppressing MMC high-frequency oscillations," *IEEE Transactions on Power Delivery*, vol. 38, no. 6, pp. 3804–3819, 2023.

[11] L. He and J. Zhang, "A community sharing market with PV and energy storage: An adaptive bidding-based double-side auction mechanism," *IEEE Transactions on Smart Grid*, vol. 12, no. 3, pp. 2450–2461, 2021.

[12] J. Lu and X. Li, "The benefits of hydrogen energy transmission and conversion systems to the renewable power grids: Day-ahead unit commitment," in *2022 North American Power Symposium (NAPS)*, pp. 1–6, 2022.

[13] C. Xie, P. Dehghanian, and A. Estebsari, "Fueling the seaport of the future: Investments in low-carbon energy technologies for operational resilience in seaport multi-energy systems," *IET Generation, Transmission & Distribution*, 2023.

[14] Z. Yang, P. Dehghanian, and M. Nazemi, "Seismic-resilient electric power distribution systems: Harnessing the mobility of power sources," *IEEE Transactions on Industry Applications*, vol. 56, no. 3, pp. 2304–2313, 2020.

[15] M. Nazemi, P. Dehghanian, X. Lu, and C. Chen, "Uncertainty-aware deployment of mobile energy storage systems for distribution grid resilience," *IEEE Transactions on Smart Grid*, vol. 12, no. 4, pp. 3200–3214, 2021.

[16] J. Su, D. Anokhin, P. Dehghanian, and M. A. Lejeune, "On the use of mobile power sources in distribution networks under endogenous uncertainty," *IEEE Transactions on Control of Network Systems*, vol. 10, no. 4, pp. 1937–1949, 2023.

[17] J. Su, S. Mehrani, P. Dehghanian, and M. A. Lejeune, "Quasi second-order stochastic dominance model for balancing wildfire risks and power outages due to proactive public safety de-energizations," *IEEE Transactions on Power Systems*, pp. 1–14, 2023.

[18] J. Su, P. Dehghanian, B. Vergara, and M. H. Kapourchali, "An energy management system for joint operation of small-scale wind turbines and electric thermal storage in isolated microgrids," in *2021 North American Power Symposium (NAPS)*, pp. 1–6, 2021.

[19] J. Su, R. Zhang, P. Dehghanian, and M. H. Kapourchali, "Pre-disaster allocation of mobile renewable-powered resilience-delivery sources in power distribution networks," in *2023 North American Power Symposium (NAPS)*, pp. 1–6, 2023.

[20] Uprise Energy, "Portability," 2023. [Online] Available at: https://upriseenergy.com/portability.

[21] M.-S. Cheon, S. Ahmed, and F. Al-Khayyal, "A branch-reduce-cut algorithm for the global optimization of probabilistically constrained linear programs," *Mathematical Programming*, vol. 108, pp. 617–634, 2006.

[22] S. Lei, J. Wang, and Y. Hou, "Remote-controlled switch allocation enabling prompt restoration of distribution systems," *IEEE Transactions on Power Systems*, vol. 33, no. 3, pp. 3129–3142, 2017.

[23] K. P. Schneider, B. Mather, B. C. Pal, C.-W. Ten, G. J. Shirek, H. Zhu, J. C. Fuller, J. L. R. Pereira, L. F. Ochoa, L. R. de Araujo, *et al.*, "Analytic considerations and design basis for the ieee distribution test feeders," *IEEE Transactions on power systems*, vol. 33, no. 3, pp. 3181–3188, 2017.

[24] P. Dehghanian and M. Kezunovic, "Probabilistic decision making for the bulk power system optimal topology control," *IEEE Transactions on Smart Grid*, vol. 7, no. 4, pp. 2071–2081, 2016.

[25] U.S. Environmental Protection Agency, "Emission factors for greenhouse gas inventories." https://www.epa.gov/sites/default/files/2018-03/documents/emission-factors_mar_2018_0.pdf, 2018.